ILASS 2008
Sep. 8-10, 2008, Como Lake, Italy

Paper ID ILASS08-4-4

DROPLET BREAKUP QUANTIFICATION AND PROCESSES IN CONSTANT AND PULSED AIR FLOWS

Majithia A. K., Hall S., Harper L., Bowen P. J.

Centre for Research in Energy, Waste and Environment, School of Engineering,
Cardiff University, 5 The Parade, Cardiff, Wales, UK, CF24 3AA

ABSTRACT
In recent years, Cardiff University has researched droplet breakup mechanisms both numerically and experimentally. This work was initially undertaken to investigate the use of water sprays in explosion suppression, but latterly the renewed interest in Pulse Detonation Engines (PDEs) and more pertinently liquid fuelled PDEs has added a further relevance to this work. This paper relates primarily to the experimental studies with water in air. High Speed Video and Laser Diagnostics have been used to characterise droplet breakup when a droplet falls under gravity into a constant air stream. The air flows were generated using basic techniques to generate low subsonic flow. When the droplet fell into a constant airflow, classical droplet breakup mechanisms were observed which included bag-breakup. Post break-up droplet sizes have been quantified, droplet size distributions and SMDs were found for several cases. The affect of viscosity has also been investigated on the induction time and the Critical Weber Number for various Ohnesorge Numbers was found and compared to previously published relations.

INTRODUCTION

There are numerous engineering applications where a knowledge of droplet break up is important. These include liquid fuelled engines and explosion suppression. It is important to know how droplets of a certain size will breakup in certain conditions so that the initial sprays can be designed appropriately.

Weber Number

Traditionally, the main parameter used to non-dimensionalise droplet breakup has been the Weber Number (We). This non-dimensional group relates the droplet's surface tension force to the aerodynamic force exerted by the ambient gas. The Weber number is given by:

$$We = \frac{\rho_a v^2 D}{\sigma} \qquad (1)$$

Much work has been done on droplet breakup and Weber Number, and the different breakup modes of a droplet have been characterised and the range of Weber Number in which they occur have been determined. Pilch and Erdman [1] recognised six modes of droplet breakup as shown in Fig. 1.

It is important to remember that the boundaries between modes are not definite, and there will be a gradual change from one mode to another.

Ohnesorge Number and Laplace Number

The Weber Number does not include the influence of viscosity. It has been suggested that the fluid viscosity can affect the mode of breakup. The Ohnesorge Number (Oh) and Laplace Number (Lp) include liquid viscosity. The Ohnesorge Number is defined as:

$$Oh = \frac{\mu_d}{\sqrt{D \rho_d \sigma}} \qquad (2)$$

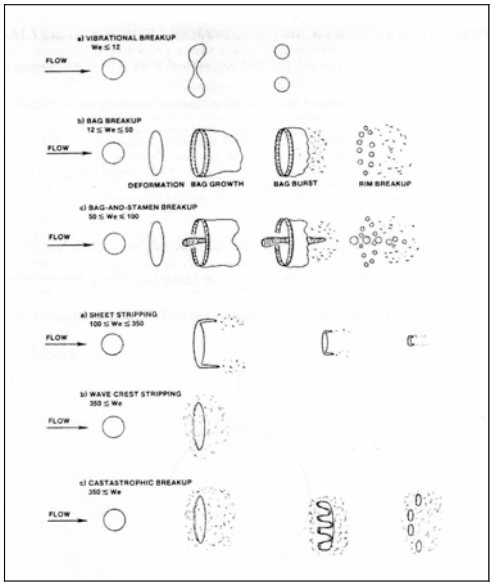

Fig. 1: Breakup Regimes

The Laplace Number is defined as:

$$Lp = \frac{1}{(Oh)^2} \qquad (3)$$

Aims

This paper looks at the different dimensionless groups that have been suggested may be important for droplet breakup. We present good quality high speed photography and size distribution results for the post breakup droplet sizes.

EXPERIMENTAL METHOD

Fig. 2 shows a schematic of the apparatus used to conduct the experiments. For post-breakup droplet sizing, the camera and light box were replaced by a Malvern Spraytec Laser Particle Sizer. Different combinations of glass nozzle/ hypodermic needle were used to generate different sized initial droplets. The airflow pipe was connected to a 7 bar central compressed air line and the flow was controlled using a regulator.

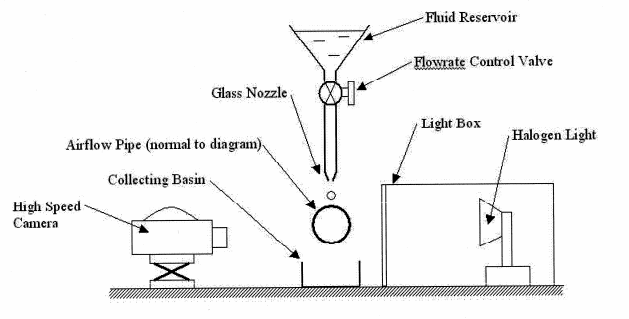

Fig. 2: Experimental Set-up

Air flow speeds were taken using a hot wire anemometer or using Laser Doppler Anemometry (LDA). Droplet sizes were calculated by pixel counting on the Photron Ultima Fastcam high speed camera images. The high speed camera recorded images at a rate of 3 000 frames/s with a shutter time of either (1/6 000) or (1/10 000) seconds.

Malvern Spraytec Particle Sizer

The Malvern Spraytec, as shown in Fig. 3, is capable of providing real-time transient spray characteristics measurement. It has a range of 2.55 – 850 µm utilising a lens with a focal length of 450 mm and has an acquisition rate of up to 10 kHz. It is connected to a PC on which the RTSizer software is installed.

Fig. 3: The Malvern Spraytec Particle Sizer

Photron Ultima Fastcam

The camera used was the Photron Ultima Fastcam APX RS Mono 16 GB. It is capable of taking images at a rate of 250,000 frames per second (fps). The images were taken at 3000 fps as this gave the maximum resolution of 1 mega-pixel.

Dantec FlowLite LDA System

The velocity profile of the nozzle was characterised using a 1D Laser Doppler Anemometry (LDA) system. LDA is a non-intrusive laser diagnostic system that allows the velocity magnitude and direction of seeded particles to be recorded. The system used is a Dantec FlowLite system operating in back scatter mode, focal length of 160 mm, beam separation of 38 mm, wavelength of 532 nm and frequency shift of 40 Mhz. The seeding particles are water droplets produced by a nebuliser in the order of 5 microns.

RESULTS AND DISCUSSION

Droplet Breakup Images and Particle Sizing

Figure 4 shows the breakup of a 3.7 mm water droplet in a flow of Weber number 14.5. According to the categorisation of Pilch and Erdman [1], the droplets should experience bag breakup. It can be seen that the droplet does experience bag breakup, but elements of the vibrational breakup mode can also be seen. Vibrational breakup occurs for We ≤ 12. The Weber number of this flow is close to this limit, and these images imply that the categorisation is not definite.

Figure 5 shows the breakup of a 3 mm water droplet in a flow of We = 20. This is an example of classical bag breakup which occurs for 12 ≤We ≤ 50 as shown in Fig. 1 [1].

Figure 6 shows a 3 mm water droplet in a flow where the Weber number is 51. This is just in the Bag-and-Stamen breakup regime (50 ≤ We ≤100, [1]). For this regime, a number of larger droplets are expected in the central region after breakup, and this appears to be the case. However, the exact breakup is not visualised in the videography.

Figure 7 and Fig. 8 are graphs show daughter droplet sizes 20 mm and 150 mm downstream of the location that the droplet falls into the airstream. At 20 mm downstream (Fig. 7), the SMD of the characterised spray is 219.84 µm and

50% of the water volume is in droplets greater than 500 µm. However, it appears that a larger amount of the spray has not been characterised due to the shape of the graphs. One would expect a normal distribution both for the Particle Size histogram and the Cumulative Under-Size graph, but this is obviously not the case.

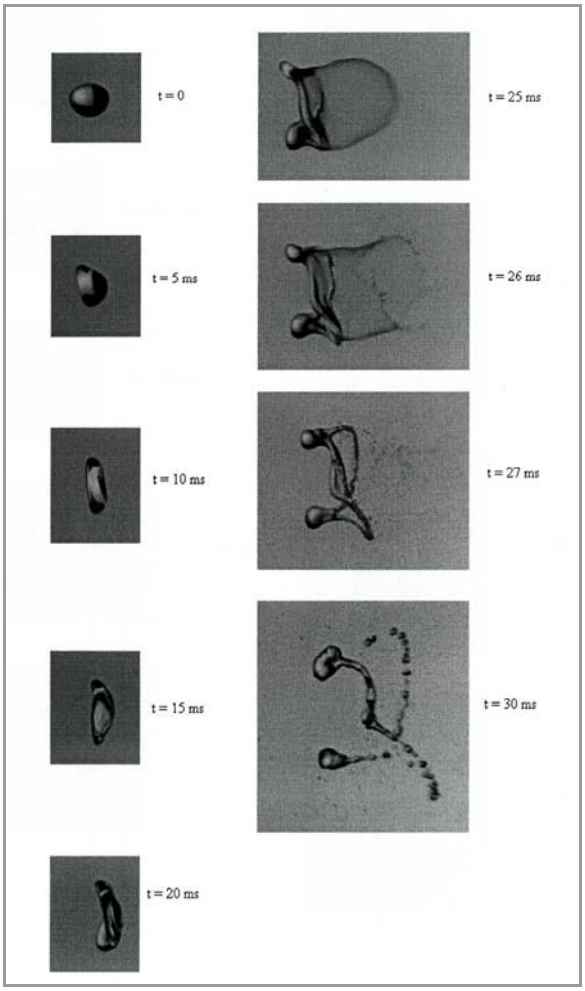

Fig. 4: Breakup of 3.7 mm Water Droplet, We = 14.5

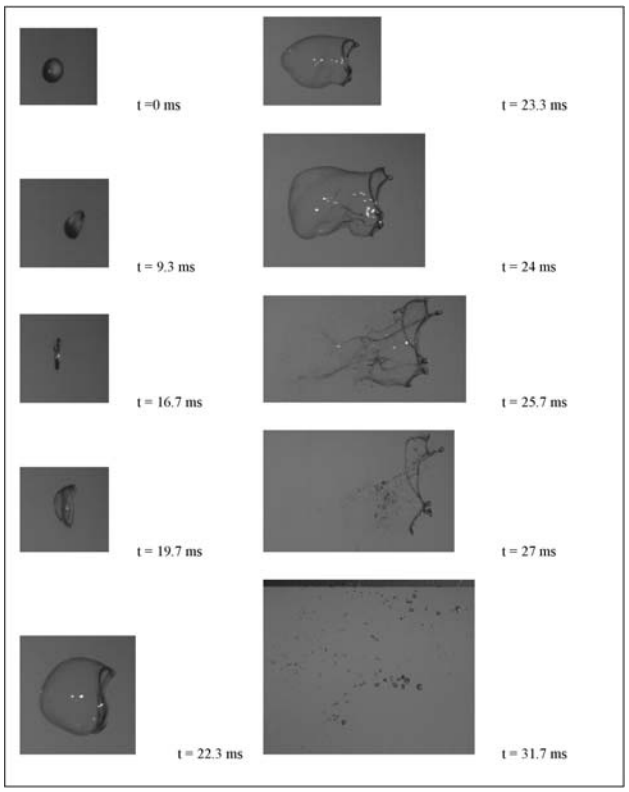

Fig. 5: Breakup of 3 mm Water Droplet, We = 20

At 150 mm downstream (Fig. 8), the graphs are more similar to those that would be expected. The SMD is still high at 217.27 µm although this is very similar to the SMD at 20 mm, while 50% of the spray is in droplets smaller than 340 µm. It is believed that the SMD for 20 mm is incorrect due to the high droplet density. For very dense sprays, the laser beam could have been diffracted through several droplets before reaching the detectors.. The reduction of the particle sizes is due to secondary breakup in the flow.

Figure 7 and Fig. 8 do not fully capture the size distribution of the secondary droplets. A normal distribution curve would be expected, and this is obviously not the case. As the data has been clipped at the top end, if the full distribution had been captured, the SMD would have increased significantly and the percentage of spray suitable for explosion suppression would have decreased markedly too.

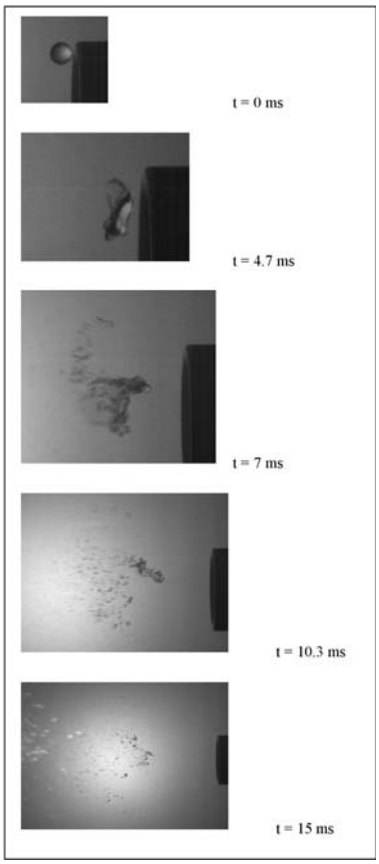

Fig 6: Breakup of 3 mm Water Droplet, We = 51

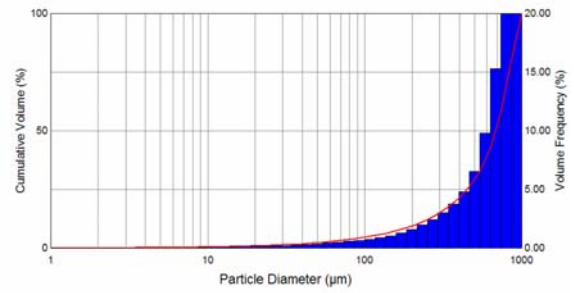

Fig. 7:Daughter Droplet Sizes, We = 51, 20 mm downstream

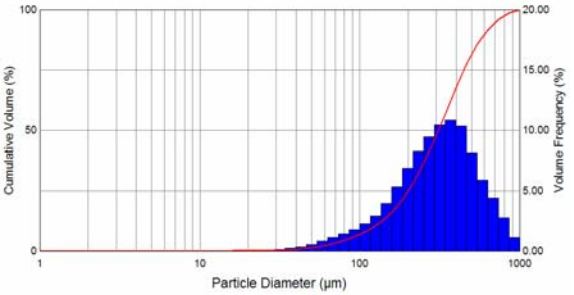

Fig. 8:Daughter Droplet Sizes, We = 51, 150 mm downstream

Figure 9 shows images for a water droplet of 3mm diameter with a Weber number of 84. The droplet appears to undergo Bag-and-Stamen breakup with possible elements of Sheet Stripping. Sheet Stripping is believed to occur in the range 100 ≤We ≤ 200 [1]. The Particle Size Histogram and Volume Undersize curve for We = 84 (Fig. 10 and Fig. 11) show similar characteristics to those for We = 51. The SMD at 20 mm downstream is 282.81 µm, while at 150 mm it is 204.81 µm. The similarity of the SMD at 150 mm downstream for We = 54 and We = 81 suggest that there is little secondary breakup. This is probably due to the decreased Weber number with respect to the secondary spray.

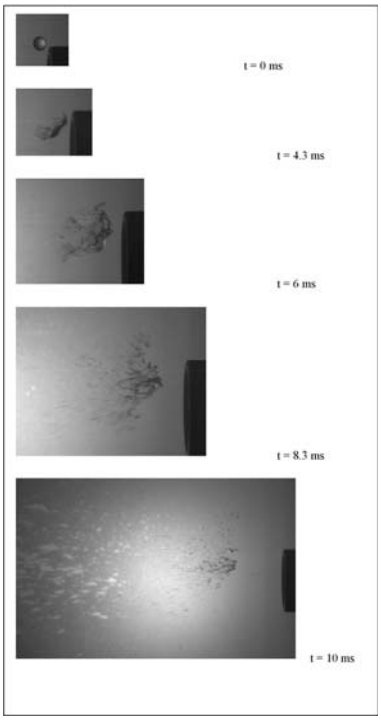

Fig 9: Breakup of 3 mm Water Droplet, We = 84

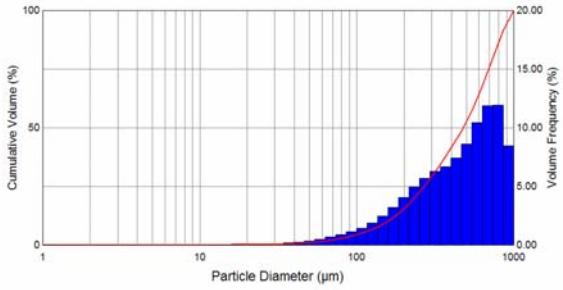

Fig. 10: Daughter Droplet Sizes, We = 84, 20 mm downstream

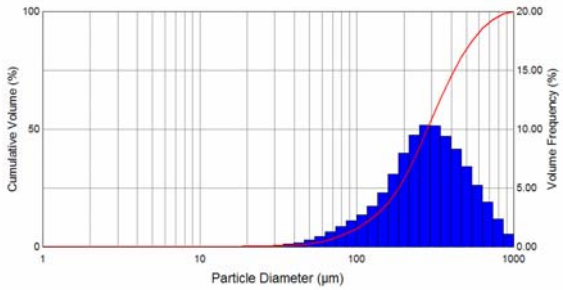

Fig. 11: Daughter Droplet Sizes, We = 84, 150 mm downstream

The images in Fig. 12 are for a slightly different configuration than the previous images. With this experiment, the air flowed from a small brass nozzle of diameter 10, whereas previously the air flowed out of a PVC nozzle with diameter 30 mm. The decreased nozzle diameter allowed increased air velocities to be achieved, although the air stream

was much narrower. The maximum air velocity measured on the nozzle centreline is 74.5 ms^{-1} using the LDA system. This equates to a Weber number of 271.4 for an initial droplet size of 3mm, which puts the flow in the "Wave Crest Stripping" region [1], and the photographic evidence supports this. Secondary droplet sizes were measured at 150 mm downstream. Figure 13 shows that the full distribution is captured, giving a large degree of confidence in the results. The SMD was found to be 17.20 µm, with 28% of the water volume in droplets of 30 µm or less which is the size of mist required for explosion suppression.

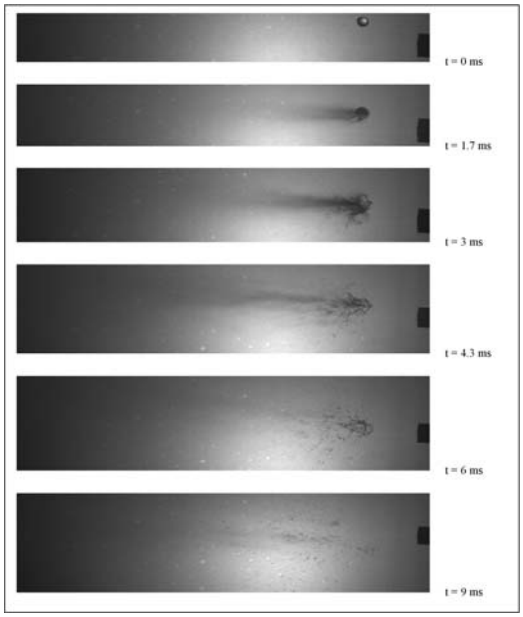

Fig. 12: Breakup of 3 mm Water Droplet, We = 271

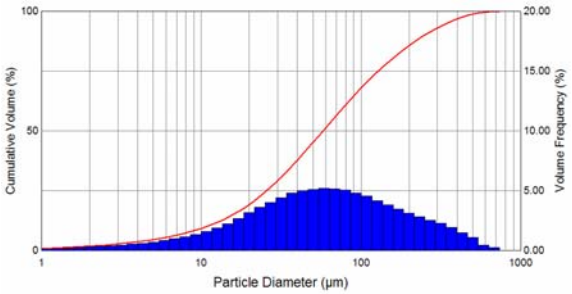

Fig. 13: Daughter Droplet Sizes, We = 271, 150 mm downstream

Critical Induction Time

The Critical Induction Time is the time between initiation and droplet breakup. However, there are various definitions of the initiation. In this paper, we take the initiation point as the time at which the droplet enters the air stream.

The Critical Induction Time is plotted against Laplace number in Fig. 14. Variations in the Laplace number were achieved by varying the viscosity by using solutions of water and glycerol in different concentrations.

The experimental results obtained are compared to Schraiber's trend for similar droplets [2]. The experimental data indicates that for high Laplace numbers, the induction time remains fairly constant, but below a certain critical Laplace number (Lp ~ 700), the induction time increases rapidly. The results do not agree well with Schraiber's curve. This could be due to the choice of initiation point for breakup or variation in the fluid properties to those calculated.

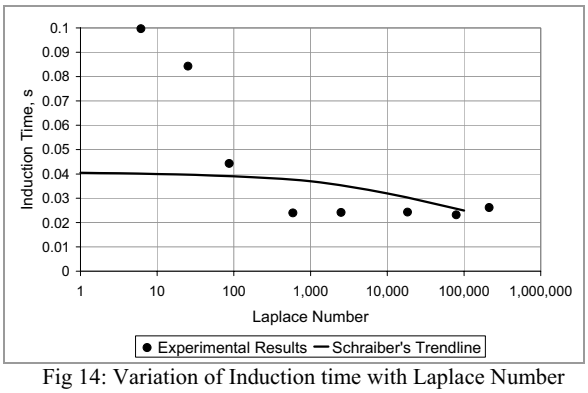

Fig 14: Variation of Induction time with Laplace Number

Supercritical Induction Time

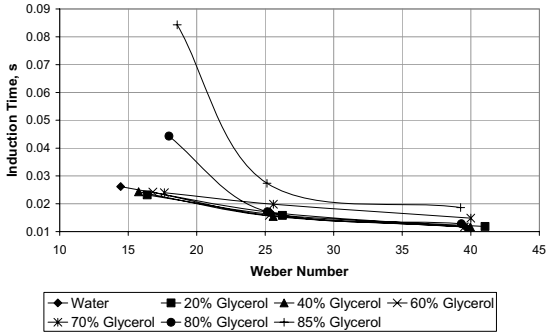

Fig 15: Induction Time for Critical and Supercritical Weber Numbers

The induction times were measured for three Weber numbers to investigate the relationship between Weber number and induction time for different mixtures (Fig. 15). With the apparatus available, a weak decrease in induction time was found with increasing Weber number, while the affect of fluid properties is not so clear. It appears that there may be a decrease in induction time with decrease in water content. It is not clear whether this is due to the increase in viscosity, increase in density or the decrease in surface tension, although the natural inference is that the decrease in surface tension has the largest affect.

Critical Weber Number

The critical Weber number was found for various Ohnesorge numbers to investigate the affect of fluid viscosity.

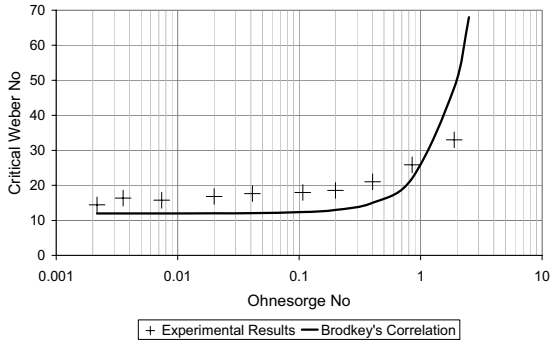

Fig 16: Variation of Critical Weber Number with Ohnesorge Number

The Critical Weber Number is the Weber Number at which the droplet starts to break up. It can be seen in Fig. 16 that the experimental Weber Number is higher than that predicted by Broadkey for lower Ohnesorge Numbers, and for higher Ohnesorge Numbers the value of the Critical Weber Number is over predicted. This may be due to the fact that the droplet did not fall into a constant velocity air flow. The velocity, for these experiments, was measured using a hot-wire anemometer, which was only accurate enough to give one velocity reading, which was chosen as the centreline. It is probable that the droplet began to break up before it reached the centreline; therefore the true Critical Weber Number is actually lower than calculated.

CONCLUSIONS

This paper presents good quality High-Speed Imagery of droplet breakup mechanisms of water in steady air flows. We have captured Bag, Bag-and-Stamen and Sheet Stripping Breakup Regimes in the appropriate Weber Number categories defined by Pilch and Erdman [1].

We have also recorded the secondary droplet sizes in these breakup regimes. Due to the equipment available, it was only possible to capture a full distribution of for the highest Weber Number of 271. However, for this Weber Number we found that 28% of the spray was sub 30 μm, which is the size required for effective explosion suppression.

We investigated the affect of viscosity on droplet breakup and found that the Critical Weber Number increases with Ohnesorge number and therefore fluid viscosity.

This paper is part of an ongoing programme of work into droplet breakup. The next stage of the work will look into how droplets breakup under pulsed flows, and will investigate the influence of Eotvos Number. This will provide a more appropriate understanding of how droplets breakup in real explosion suppression environments and in Pulse Detonation Engines.

NOMENCLATURE

Symbol	Quantity	S.I. Unit
Latin Symbols		
D	Diameter	m
Lp	Laplace Number	Dimensionless
Oh	Ohnesorge Number	Dimensionless
We	Weber Number	Dimensionless
v	Relative Velocity	m s^{-1}
Greek Symbols		
μ	Absolute Viscosity	N s m^{-2}
ρ	Density	kg m^{-3}
σ	Surface Tension	N m^{-1}
Subscripts		
a	Air	
d	Droplet	

REFERENCES

[1] M. Pilch and C. A. Erdman, Use of Breakup Time Data and Velocity History Data to Predict the Maximum Size of Stable Fragments for Acceleration-Induced Breakup of a Liquid Drop, *Int. J. Multiphase Flow*, vol. 13, pp 741-757, 1987.

[2] A. A. Shraiber, A. M. Podvysotsky and V. V. Dubrovsky, Deformation and Breakup of Drops by Aerodynamic Forces, *Atomization and Sprays*, vol. 6, pp 667-692, 1996.

[3] L. Harper, Droplet Deformation and Breakup, BEng Project Report, Cardiff University, 2006.

[4] S. Hall, Droplet Deformation and Breakup, BEng Project Report, Cardiff University, 2007.